



OPEN Construction of cuproptosis-related genes risk model predicts the prognosis of Uterine Corpus Endometrial Carcinoma

Yanfang Huang^{1,5}, Guoxian Luo^{2,5}, Xiujie Sheng³ & Jianqi Li^{3,4}✉

Cuproptosis, a recently discovered form of cell death, has emerged as a crucial player in tumor development, although its role in uterine corpus endometrial carcinoma (UCEC) remains inadequately explored. This study aims to identify prognostically relevant cuproptosis-related genes in endometrial cancer. Cuproptosis-related genes were sourced from previously published studies and the FerrDb database. UCEC gene expression profiles and clinical data were obtained from the TCGA database. Differential gene expression was determined using LIMMA analysis, and functional enrichment analysis was conducted on identified cuproptosis-related genes. A prognostic model for UCEC was developed using LASSO Cox regression analysis and a Nomogram, integrating survival data, status, and gene signatures. TIMER analysis assessed the impact of crucial cuproptosis-related genes on immune cell infiltration in UCEC. Validation of the selected genes, CDKN2A, GLS, and PPAT, was performed at both mRNA and protein levels. A total of 27 cuproptosis-related genes were identified, with 19 upregulated and 6 downregulated in UCEC. These genes were associated with key signaling pathways, including the TCA cycle, Pyruvate metabolism, Glycolysis/Gluconeogenesis, and Platinum drug resistance. The LASSO regression and Nomogram models demonstrated robust predictive performance for UCEC prognosis, identifying CDKN2A, GLS, and PPAT as critical prognostic genes. Furthermore, these genes played essential roles in immune cell infiltration in UCEC, confirming their significance. Validation at both mRNA and protein levels solidified the role of CDKN2A, GLS, and PPAT. The identified signature of CDKN2A, GLS, and PPAT demonstrates significant predictive value for UCEC prognosis, suggesting their potential as therapeutic targets, including their application in immunotherapy strategies.

Keywords Cuproptosis, Ferroptosis, Uterine Corpus Endometrial Carcinoma, GLS, Prognostic

Endometrial cancer, one of the most prevalent malignancies in the female reproductive system, ranks second in incidence among such tumors in China and first in the United States and other Western developed nations^{1–3}. While incidence rates have either increased or stabilized globally over the past decade, notable surges are evident in South Africa and several Asian countries⁴. Despite these trends, patients with poorly differentiated and locally advanced tumors face inevitable metastasis and postoperative recurrence, often leading to mortality^{5,6}. This highlights an urgent need for a deeper exploration of the molecular mechanisms underlying endometrial cancer development, particularly in the context of cell death. The identification of novel candidate genes is imperative to enhance early diagnosis and inform treatment decisions.

An increasing number of novel non-apoptotic forms of regulated cell death (RCD) have been identified, including necroptosis, pyroptosis, ferroptosis, endocytic cell death, reticulocyte death, parthanatos, lysosome-

¹Department of Anesthesiology, Guangzhou First People's hospital;The First People's Hospital of Guangzhou Medical University, The Second Affiliated Hospital of South China University of Technology, Guangzhou 510000, China. ²Department of Gynecology, The Fourth Affiliated Hospital of Guangzhou Medical University, Guangzhou 510000, China. ³Department of Obstetrics and Gynecology, Guangdong Provincial Key Laboratory of Major Obstetric Diseases, Guangdong Provincial Clinical Research Center for Obstetrics and Gynecology, Laboratory of Maternal-Fetal Medicine, The Third Affiliated Hospital, Guangzhou Medical University, Guangdong-Hong Kong-Macao Greater Bay Area Higher Education Joint, Guangzhou 510000, China. ⁴Department of Obstetrics and Gynecology, Guangdong Province Key Laboratory of Major Obstetric Diseases, The Third Affiliated Hospital, Guangzhou Medical University, No.63 DuoBao Road, Guangzhou 510000, Guangdong, P.R. China. ⁵Yanfang Huang and Guoxian Luo contributed equally. ✉email: 2014683021@gzhmu.edu.cn

dependent Sexual cell death, autophagy-dependent cell death, alkaline cell death, and hypoxia⁷. Understanding and applying these RCD mechanisms could lead to discovering new therapeutic targets and provide rich means for diagnosing and treating tumors.

In March 2022, a landmark publication in SCIENCE described a newly characterized mechanism of cell death, distinct from previously known RCD pathways. This mechanism, termed “cuproptosis,” was elucidated by Tsvetkov et al. Through their analysis of phenomena, mechanisms, and disease models, the researchers found that copper directly binds to the fatty acylation components of the tricarboxylic acid cycle (TCA), leading to the aggregation of fatty acylated proteins and the loss of iron-sulfur cluster proteins, which in turn trigger proteotoxicity stress and eventually lead to cell death⁸.

There is increasing evidence that copper is involved in tumor cell initiation and progression. However, research on the role of cuproptosis-related genes in the progression and prognosis of UCEC remains limited. Therefore, this study aims to explore the role of cuproptosis-related genes in UCEC by constructing a predictive model, with the goal of identifying potential prognostic markers for UCEC.

Materials and methods

UCEC gene expression data and clinical data acquisition

The TCGA-UCEC data set and clinical information were downloaded from the Cancer Genome Atlas (TCGA) database. The Sangerbox online analysis tool was used for data standardization and transformation. Samples with absent, repeated, missing, or severely incorrect gene expression information were excluded. A summary of the clinical information is provided in Table 1.

Acquisition of cuproptosis-related genes

Cuproptosis-related genes were identified from a seminal article published in SCIENCE on cuproptosis. Using the FerrDb database (<http://www.zhounan.org/ferrdb>), 27 cuproptosis-related genes were curated. Unlike previous studies, our research incorporated an additional 17 cuproptosis-related genes, establishing a robust foundation for subsequent analysis (Table S1).

Identification of UCEC differentially expressed genes and cuproptosis-related genes

Differentially expressed genes (DEGs) between UCEC and normal endometrial tissue samples were identified using the LIMMA R package. Based on these results, expression profiles of 27 cuproptosis-related genes were analyzed.

Functional enrichment analysis of cuproptosis-related genes

Gene Ontology (GO) annotations and Kyoto Encyclopedia of Genes and Genomes (KEGG) pathway analyses were conducted using online tools (www.kegg.jp/kegg/kegg1.html). Permission from the Kanehisa laboratory was obtained for tool usage.

Characteristics	Alive(N= 449)	Dead(N= 87)	Total(N= 536)	pvalue	FDR
Age					
Mean ± SD	63.36 ± 11.02	66.69 ± 10.85	63.90 ± 11.05		
Median[min-max]	63.00[31.00,90.00]	67.00[35.00,88.00]	64.00[31.00,90.00]		
BMI					
Mean ± SD	33.59 ± 9.15	32.74 ± 8.81	33.45 ± 9.09		
Median[min-max]	32.42[17.36,81.64]	31.62[18.07,61.03]	32.21[17.36,81.64]		
Histological type				2.10E-06	4.30E-06
Endometrioid	354(66.04%)	46(8.58%)	400(74.63%)		
Mixed	16(2.99%)	6(1.12%)	22(4.10%)		
Serous	79(14.74%)	35(6.53%)	114(21.27%)		
Stage				3.40E-12	1.00E-11
Stage I	304(56.72%)	29(5.41%)	333(62.13%)		
Stage II	42(7.84%)	9(1.68%)	51(9.51%)		
Stage III	90(16.79%)	33(6.16%)	123(22.95%)		
Stage IV	13(2.43%)	16(2.99%)	29(5.41%)		
Grade				5.00E-06	5.00E-06
G1	95(17.72%)	2(0.37%)	97(18.10%)		
G2	105(19.59%)	14(2.61%)	119(22.20%)		
G3	249(46.46%)	71(13.25%)	320(59.70%)		

Table 1. The clinical information for TCGA UCEC dataset.

Construction of LASSO model

The Least Absolute Shrinkage and Selection Operator (LASSO)-Cox regression model was constructed using the R package “glmnet.” Survival time, survival status, and expression levels of 27 cuproptosis-related genes were integrated into the model.

Multivariate survival analysis and Kaplan-Meier survival curves

Survival data were analyzed using the R package “survival”. The prognostic significance of individual genes was assessed through Cox regression. The optimal RiskScore cutoff value was determined using the “maxstat” package, setting minimum and maximum grouping sample proportions to >25% and <75%, respectively. Patients were stratified into high-risk and low-risk groups. Prognostic differences between groups were evaluated using the log-rank test.

Construction of the Nomogram model

To predict outcome risks, a Nomogram was constructed using the R package “rms.” Data from survival time, survival status, and eight features (age, BMI, stage, grade, essential cuproptosis-related genes, and risk score) were integrated, and prognostic significance was assessed across 536 samples.

Immune infiltration analysis of cuproptosis-related genes

Unified and standardized pan-cancer datasets from UCSC Xena (<https://xenabrowser.net/>) were utilized. Three cuproptosis-related genes' expression data were extracted, and their relationships with six immune cell infiltration scores were analyzed using the TIMER database. Additionally, Pearson's correlation coefficients between these genes and immune infiltration scores in UCEC were calculated using the R package “psych” (version 2.1.6).

Validation of cuproptosis-related gene expression

To validate mRNA and protein expression of CDKN2A, GLS, and PPAT, quantitative real-time PCR (qPCR) and Western blot analyses were conducted on 30 UCEC and normal endometrial tissue pairs.

Sample size estimation is based on predetermined effect size (d), significance level ($\alpha = 0.05$), and statistical power ($\beta = 0.80$). The sample size of 60 (30 per group) exceeds these requirements^{9,10}.

$$n = \frac{2 \cdot (Z_{\alpha/2} + Z_{\beta})^2 \cdot \sigma^2}{\Delta^2}$$

- n: Required sample size for each group.
- Δ : Expected mean difference between groups.
- σ : Standard deviation.
- $Z_{\alpha/2}$ and Z_{β} : Z-scores corresponding to the significance level and statistical power (1.96 and 0.84, respectively).

qPCR procedure

Total RNA was extracted using Trizol reagent, followed by reverse transcription with the Revert Aid First-Strand cDNA Synthesis Kit. qPCR was performed using the SYBR Premix Ex Taq II Kit. GAPDH served as the endogenous control, and relative mRNA expression was calculated using the $2^{-\Delta\Delta Cq}$ method. Each sample was analyzed in triplicate.

Western blot procedure

Protein supernatants were separated via 10% SDS-PAGE and transferred to PVDF membranes. Membranes were blocked with 5% milk and incubated with primary antibodies (CDKN2A, GLS, PPAT, and GAPDH) overnight at 4 °C. Horseradish peroxidase-conjugated secondary antibodies were applied, and visualization was achieved with ECL chromogenic substrate reagent. Semi-quantitative analysis was performed using Image J, with GAPDH as the reference.

Results

Expression profiles of 27 cuproptosis-related genes derived from UCEC differentially expressed genes

From 536 cases of UCEC and 11 cases of normal endometrium tissue, a total of 2,516 differentially expressed genes were identified by LIMMA analysis, including 1,107 upregulated genes and 1,409 downregulated genes (Fig. 1A and B). Further analysis of these results yielded the expression profiles of 27 cuproptosis-related genes. Among these, 19 genes were upregulated (FDX1, DLAT, PDHA1, PDHB, SLC31A1, CDKN2A, DNA2, NTHL1, POLE, POLD1, CISD1, GLRX5, PPAT, ELP3, CDK5RAP1, ISCA2, ETFDH, HSPA1B, and ATP7B), while 6 genes were down-regulated (LIAS, LIPT1, MTF1, GLS, HSPA1A, and ATP7A). Two genes, DLD and RTEL1, showed no significant differences in expression (Fig. 1C).

Functional enrichment analysis of 27 cuproptosis-related genes

Using KEGG Pathway annotations and GO annotations, we identified significant enrichment in pathways such as the TCA cycle, Pyruvate metabolism, Glycolysis/Gluconeogenesis, Platinum drug resistance, and Carbon metabolism (Fig. 2A). Additionally, these genes were involved in functions including iron-sulfur cluster binding, metal cluster binding, copper ion transmembrane transporter activity, and copper ion import (Fig. 2B).

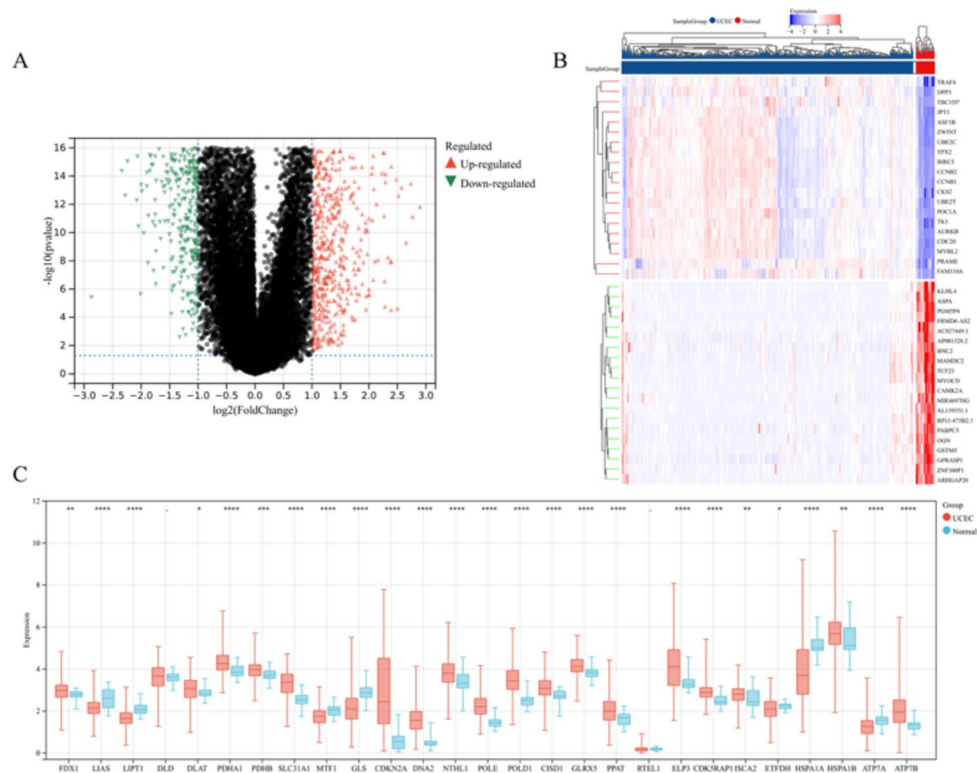


Fig. 1. Expression profiles of differentially expressed genes and cuproptosis-related genes in UCEC. (A). The UCEC differentially expressed gene volcano map, calculated by 2-fold differential expression, showed 1 107 up-regulated genes and 1 409 down-regulated genes. (B). Heat map of differentially expressed genes in UCEC. (C). Expression profiles of 27 cuproptosis-related genes in UCEC, including 19 up-regulated genes, 6 down-regulated genes, and 2 genes with no difference.

Construction of the LASSO-COX model

A LASSO-COX model was developed using the R package “glmnet” by integrating survival time, survival status, and expression data of 27 cuproptosis-related genes (Fig. 3A). The optimal Lambda value of 0.023 was used, resulting in the selection of six genes. The model formula is as follows (Fig. 3C):

$$\begin{aligned} \text{RiskScore} = & 0.0099 * \text{PDHA1} \\ & + 0.1906 * \text{GLS} \\ & + 0.1684 * \text{CDKN2A} \\ & + 0.0673 * \text{PPAT} \\ & + 0.0543 * \text{CDK5RAP1} \\ & + 0.0527 * \text{ATP7B} \end{aligned}$$

The final area under the curve (AUC) values obtained via ROC analysis were 0.61 at 365 days, 0.70 at 1095 days, and 0.71 at 1825 days, demonstrating the model’s reliability (Fig. 3B). Using an optimal cutoff value of 1.5187, patients were classified into high-risk and low-risk groups. Significant differences in prognosis between these groups were identified ($P = 7.0e^{-10}$) using the log-rank test (Fig. 3D).

LASSO heatmap and multivariate analysis

Risk scores were analyzed alongside patients’ follow-up times, events, and gene expression profiles. Increasing risk scores corresponded with decreased survival rates in UCEC patients (Fig. 4A). A heatmap of OS-related CRGs expression was generated. Multivariate Cox regression identified six key cuproptosis-related genes (GLS, CDKN2A, PPAT, PDHA1, CDK5RAP1, and ATP7B) significantly associated with survival (Fig. 4B).

KM survival curves of six cuproptosis-related genes

Kaplan-Meier survival curves indicated that three genes (CDKN2A: $P = 2.4e^{-4}$, GLS: $P = 2.5e^{-3}$, and PPAT: $P = 2.5e^{-3}$) were significantly associated with prognosis (Fig. 5A-F). Among these, high-risk groups consistently showed worse prognoses. CDKN2A, GLS, and PPAT were identified as potential prognostic biomarkers for UCEC. Subgroup analyses across age and BMI categories revealed consistent trends (Fig. 6).

Construction and assessment of the Nomogram

A Nomogram was constructed to predict 1-, 3-, and 5-year survival probabilities based on age and risk scores (Fig. 7A). The model exhibited strong performance, with a concordance index of 0.785 (95% CI: 0.735–0.835,

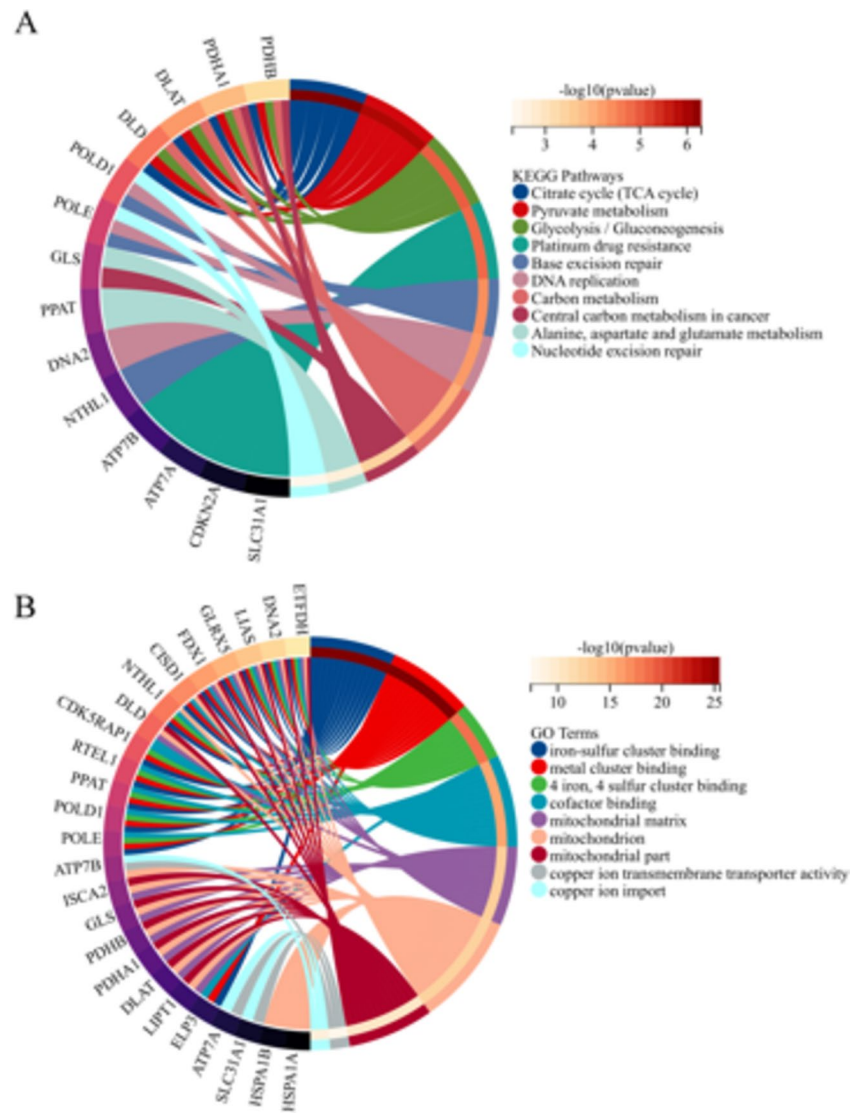


Fig. 2. Functional enrichment analysis of 27 cuproptosis-related genes. (A). KEGG Pathway of 27 cuproptosis-related genes. (B). GO annotation of 27 cuproptosis-related genes.

$P = 4.10e^{-29}$). Calibration curves indicated high consistency between predicted and observed survival times (Fig. 7B).

Functional enrichment analysis of three key cuproptosis-related genes

Functional analysis of CDKN2A, GLS, and PPAT revealed their involvement in pathways such as the TCA cycle, Pyruvate metabolism, and Platinum drug resistance. Their roles in molecular functions like iron-sulfur cluster binding and metal cluster binding were also noted (Fig. 8). Protein-protein interaction analysis demonstrated a co-expression network among the three genes.

Immune infiltration analysis of three key cuproptosis-related genes

Immune infiltration analysis indicated a negative correlation between CDKN2A expression and CD8+ T cell invasion scores, but positive correlations with CD4+ T cells and dendritic cells. GLS expression correlated positively with neutrophils and dendritic cells and negatively with macrophages. PPAT expression correlated positively with dendritic cells and negatively with B cells and macrophages (Fig. 9A-C). Overall, the three genes were significantly associated with immune infiltration levels in UCEC (Fig. 9D-F).

Validation of mRNA and protein expression levels of three key cuproptosis-related genes

Quantitative PCR and Western blot analyses were conducted on 30 pairs of UCEC and normal endometrial tissues. The mRNA levels of CDKN2A, GLS, and PPAT were significantly different between UCEC and normal tissues (Fig. 10A). Similarly, their protein levels showed significant differences, confirming their potential as prognostic markers (Fig. 10B-E).

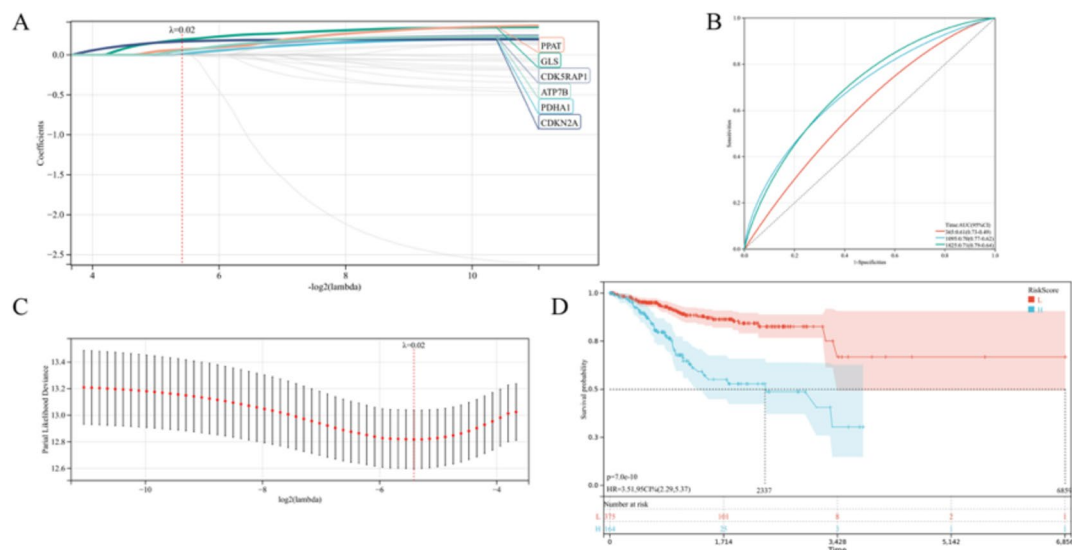


Fig. 3. Lasso-cox regression analysis results. (A). The lasso-cox optimal model obtained 6 cuproptosis-related genes, namely GLS, CDKN2A, PPAT, PDHA1, CDK5RAP1, and ATP7B. (B). ROC analysis to obtain the AUC curve. (C). Lasso-cox regression analysis sets the Lambda value to 0.0234. (D). The prognosis of the high RiskScore group and the low RiskScore group showed a significant difference ($P = 7.0e^{-10}$), and the best cut-off value of RiskScore was 1.5187.

Discussion

Cuproptosis, a newly identified form of regulated cell death characterized by the accumulation of copper ions and their interaction with mitochondrial components, has emerged as a compelling focus in cancer research. Studies have confirmed the role of copper in promoting angiogenesis, a critical process in tumor progression and metastasis, through the activation of factors such as angiopoietin, VEGF, FGF-1, and IL-1. Copper also stabilizes HIF-1 α , enhancing the expression of pro-angiogenic molecules, thereby promoting tumor proliferation and invasion^{11–14}. These findings highlight Copper's integral role in cancer biology, making it a potential therapeutic target for cancer treatment and prevention¹⁵.

First introduced in *Science*, cuproptosis delineates its unique mechanisms from other cell death pathways and highlights a set of associated genes, offering a novel paradigm for cancer research⁸. Building on this foundation, Li et al. revealed an association between a high cuproptosis index and advanced hepatocellular carcinoma, emphasizing its role in tumor aggressiveness¹⁶. Song et al. successfully applied a cuproptosis scoring system to predict bladder cancer prognosis and immune responses, indicating its broader utility in oncology¹⁷.

Gene expression profiles of TCGA-UCEC were analyzed in combination with 27 cuproptosis-related genes from the FerrDb database, providing a robust framework for studying endometrial cancer. Functional enrichment analysis revealed that these genes are involved in crucial pathways such as the TCA cycle, glycolysis/gluconeogenesis, and metal ion transmembrane transporter activity. These pathways underscore the critical role of Copper and its related genes in endometrial cancer development. By constructing a LASSO Cox regression model, six genes were identified as prognostic markers, and three key genes—CDKN2A, GLS, and PPAT—were further validated at both mRNA and protein levels, affirming their significance in UCEC prognosis.

While CDKN2A is established as a regulator of cell cycle checkpoints and autophagy^{18,19}, GLS plays a crucial role in glutamine metabolism, supporting tumor growth^{20,21}. However, the role of PPAT in UCEC remains unexplored, representing an exciting avenue for future studies. Additionally, our findings align with prior work demonstrating the prognostic significance of CDKN2A and GLS but uniquely emphasize their potential interplay within the context of cuproptosis.

Notably, this study's approach integrates advanced bioinformatics tools to provide a comprehensive analysis of cuproptosis-related pathways and their impact on UCEC. The combination of KEGG pathway analysis, gene ontology annotations, and prognostic modeling offers novel insights into the role of cuproptosis in cancer.

Unlike previous studies relying on limited gene sets, our approach utilized a broader dataset from FerrDb, encompassing 27 genes to improve model accuracy. Previous studies have utilized limited gene sets, such as the 13 cuproptosis-related genes directly derived from the SCIENCE article^{22,23}, which may constrain the scope of research. In contrast, our use of the FerrDb database expanded the gene set to 27, enhancing model precision and allowing for a broader exploration of cuproptosis-related mechanisms. Notably, while some studies identified different genes like LIPT1 as relevant to UCEC²², the absence of LIPT1 in our analysis may reflect disparities in methodological frameworks or gene set definitions. This highlights the need for standardized datasets and cross-study validations to ensure reproducibility. Another notable aspect of this study is its methodological rigor. Unlike some prior analyses that relied solely on WGCNA for differential gene selection²³, we incorporated functional enrichment analyses and Nomogram modeling to ensure a robust prognostic model.

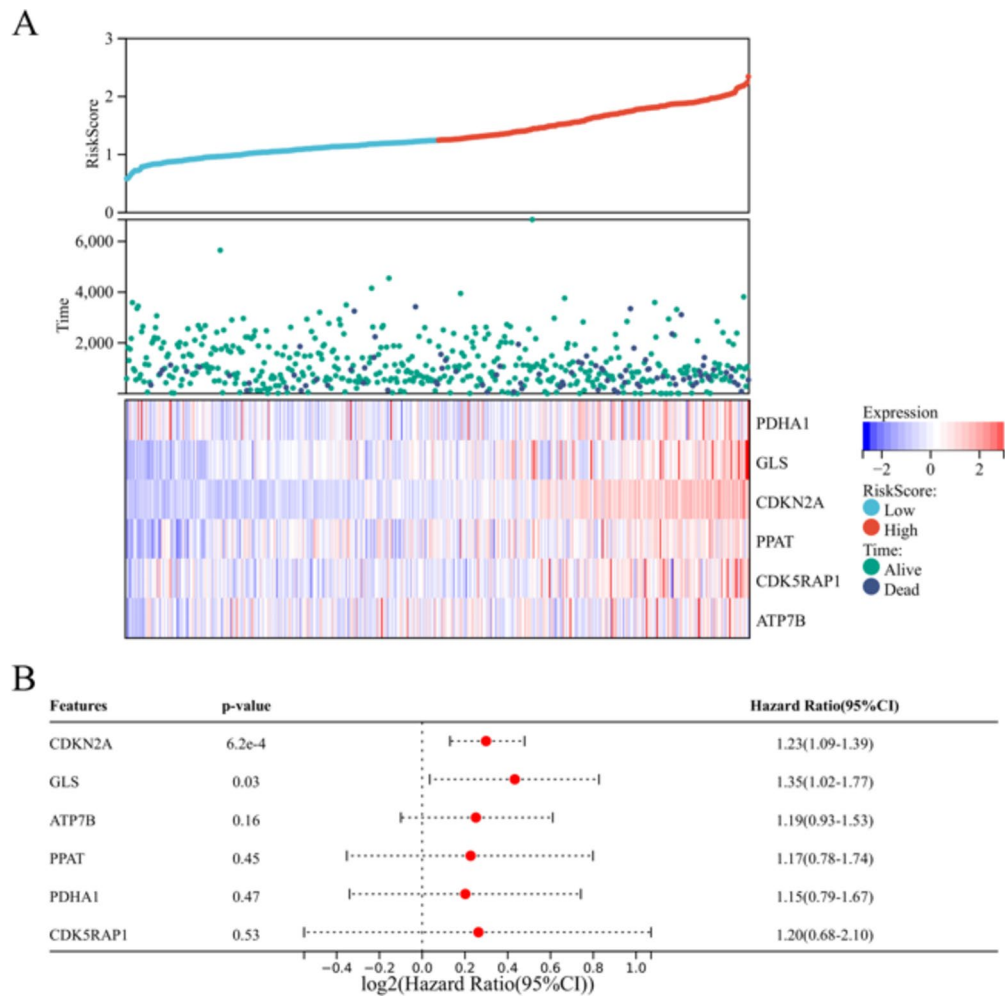


Fig. 4. Lasso-cox regression analysis expression heat map and multivariate analysis. **(A).** Lasso-cox regression analysis expression heat map. **(B).** Multivariate analysis of forest plot. Multivariate Cox regression showing 6 cuproptosis-related genes (GLS, CDKN2A, PPAT, PDHA1, CDK5RAP1, and ATP7B) associated with OS in UCEC.

The Nomogram model offers several advantages over WGCNA in bioinformatics analysis. Nomograms integrate gene features with clinical variables (e.g., age, tumor stage) to create a quantifiable and intuitive prediction tool. Using methods like LASSO regression, Nomograms efficiently select key variables, avoiding multicollinearity and overfitting. Moreover, the predictive performance of Nomograms can be validated using metrics like the concordance index (C-index) and calibration curves, providing results with higher clinical applicability. In contrast, WGCNA primarily identifies gene co-expression modules and their correlation with phenotypes. While it reveals potential biological mechanisms, it lacks direct predictive capabilities and often requires additional analysis for clinical application. Previous studies show that WGCNA's complex networks and module analyses are better suited for exploratory research. In comparison, Nomograms, with their intuitive risk scoring and robust validation systems, provide a rapid and efficient tool for clinical translation. Thus, Nomograms are widely used in cancer prognosis model construction, contributing significantly to precision medicine. Comparative evaluations reveal that Nomogram modeling provides quantifiable and clinically applicable results, outperforming WGCNA in predictive precision and risk stratification^{24,25}.

Nevertheless, despite the strengths of our bioinformatics approach, we noted that the racial and regional distribution of TCGA-UCEC database samples might contribute to variability in gene expression results. And we acknowledge the absence of *in vivo* and *in vitro* validation experiments, which are crucial for translating our findings into clinical applications. Future studies should incorporate functional validation of identified biomarkers to strengthen their clinical applicability.

In conclusion, this study advances the understanding of cuproptosis in UCEC by identifying novel prognostic biomarkers and providing a framework for further research. However, the biological mechanisms underlying cuproptosis in UCEC, particularly involving PPAT, require additional experimental exploration to uncover potential therapeutic strategies.

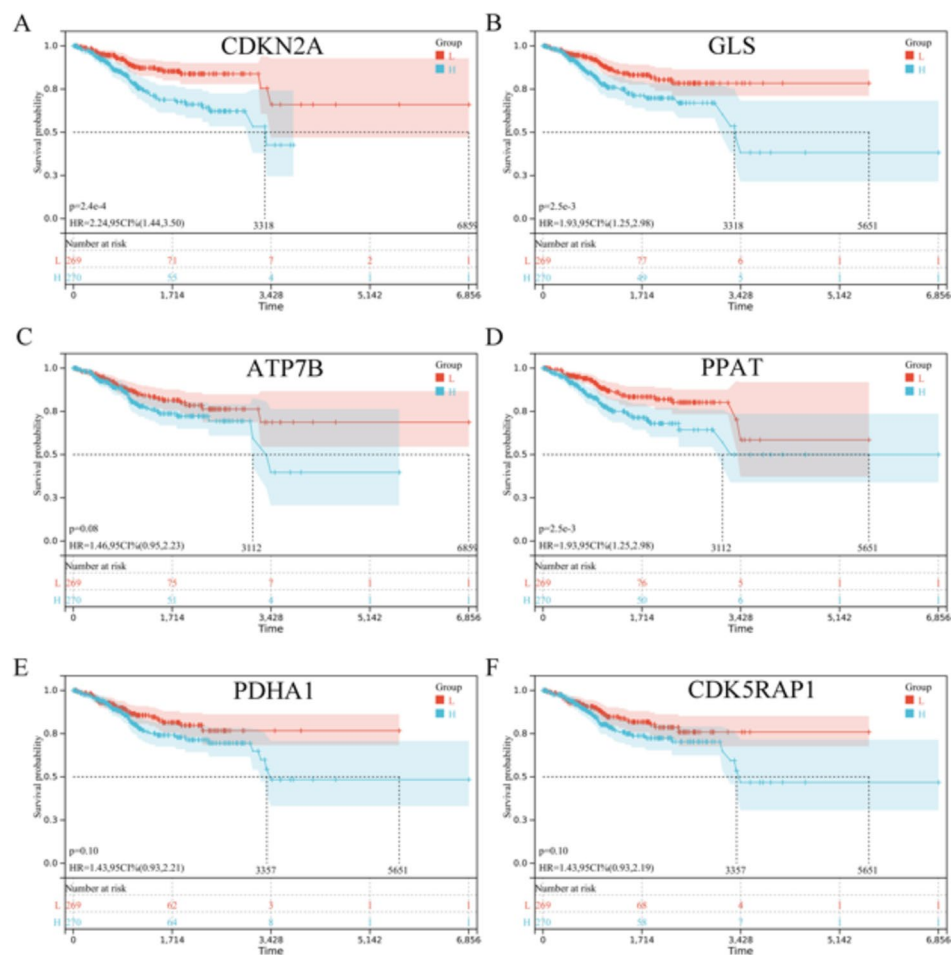


Fig. 5. Survival rates of UCEC patients with high-risk and low-risk patients with UCEC in 6 cuproptosis-related genes. (A). KM curve of CDKN2A, $P = 2.4 \times 10^{-4}$. (B). KM curve of GLS, $P = 2.5 \times 10^{-3}$. (C). KM curve of ATP7B, $P = 0.08$. (D). KM curve of PPAT, $P = 2.5 \times 10^{-3}$. (E). KM curve for DHA1, $P = 0.10$. (F). KM curves of CDK5RAP1, $P = 0.10$.

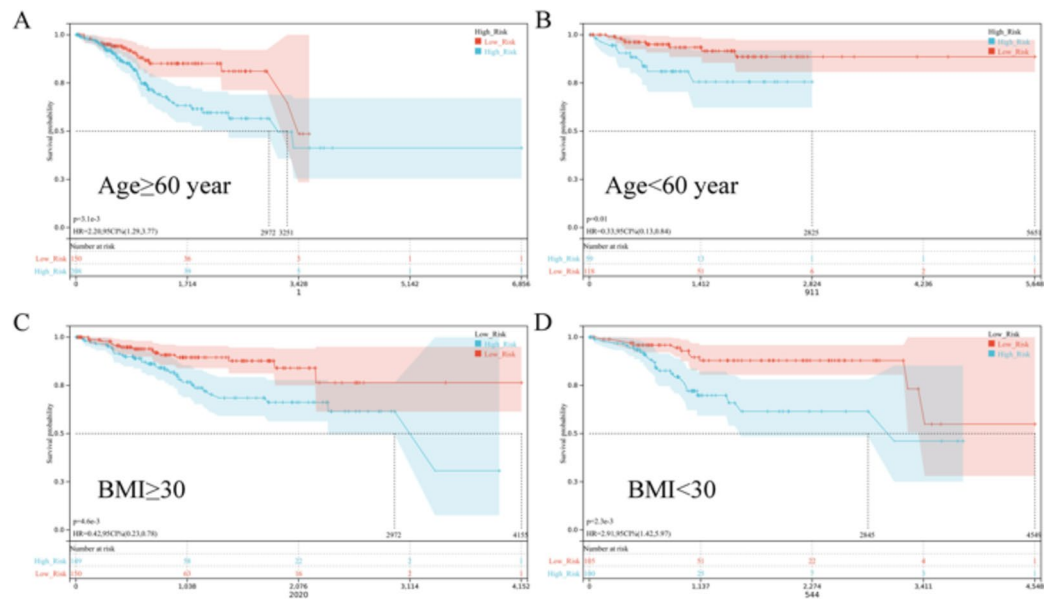


Fig. 6. Survival rates of UCEC patients with high and low-risk patients with UCEC in the subgroups based on clinicopathological characteristics. **(A)** The subgroup of age ≥ 60 years. **(B)** The subgroup of age < 60 years. **(C)** The subgroup of BMI ≥ 30 . **(D)** The subgroup of BMI < 30.

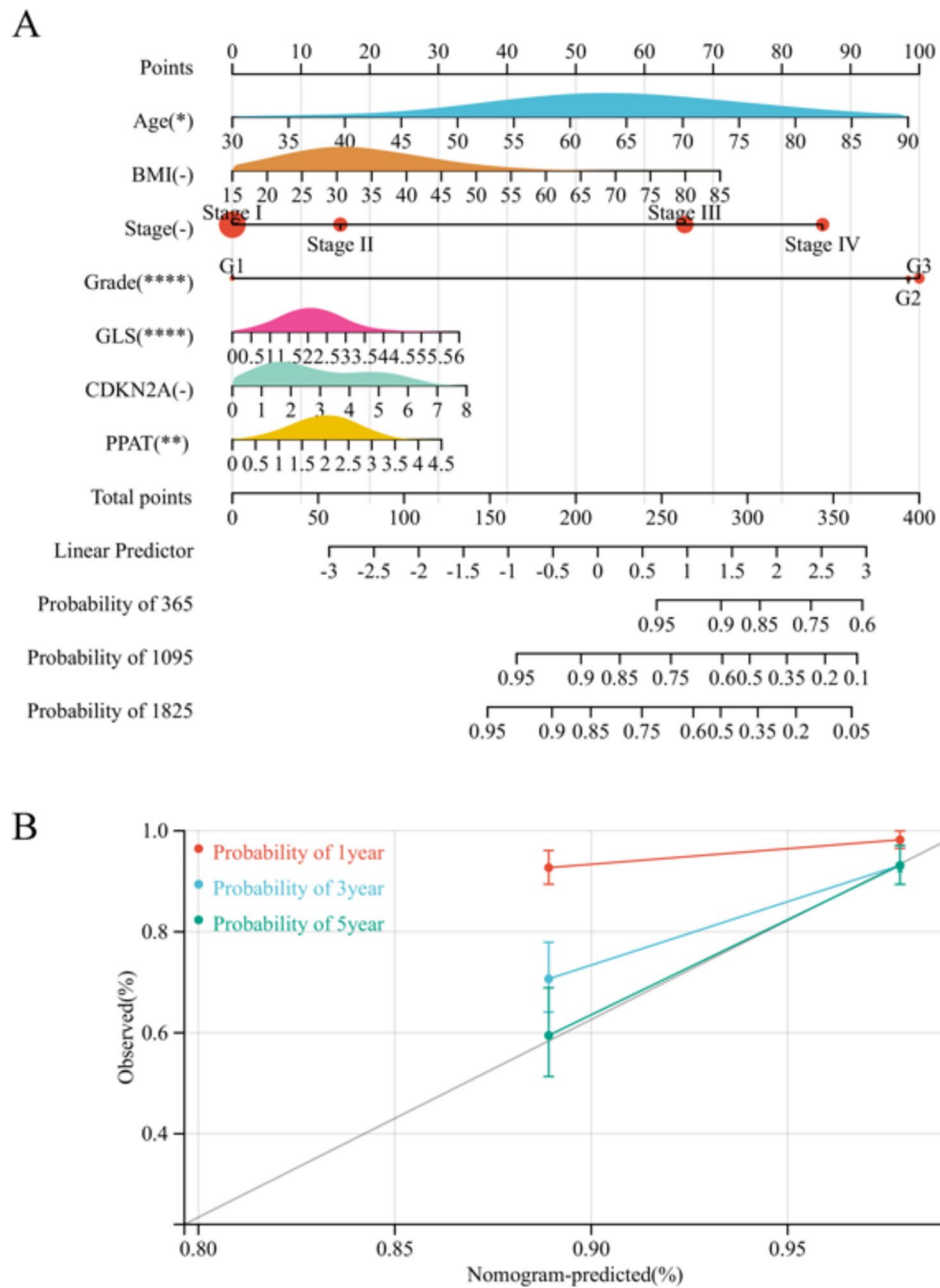


Fig. 7. Establishment of the nomogram prediction model. **(A)** A prognostic nomogram based on the risk score using the age, BMI, stage, grade, and prognostic cuproptosis-related genes signature (CDKN2A, GLS, and PPAT) to predict 1-, 3-, and 5-year survival in patients with UCEC. **(B)** Calibration curves corrected for deviations in agreement between the predicted and observed survival rates at 1-, 3-, and 5 years.

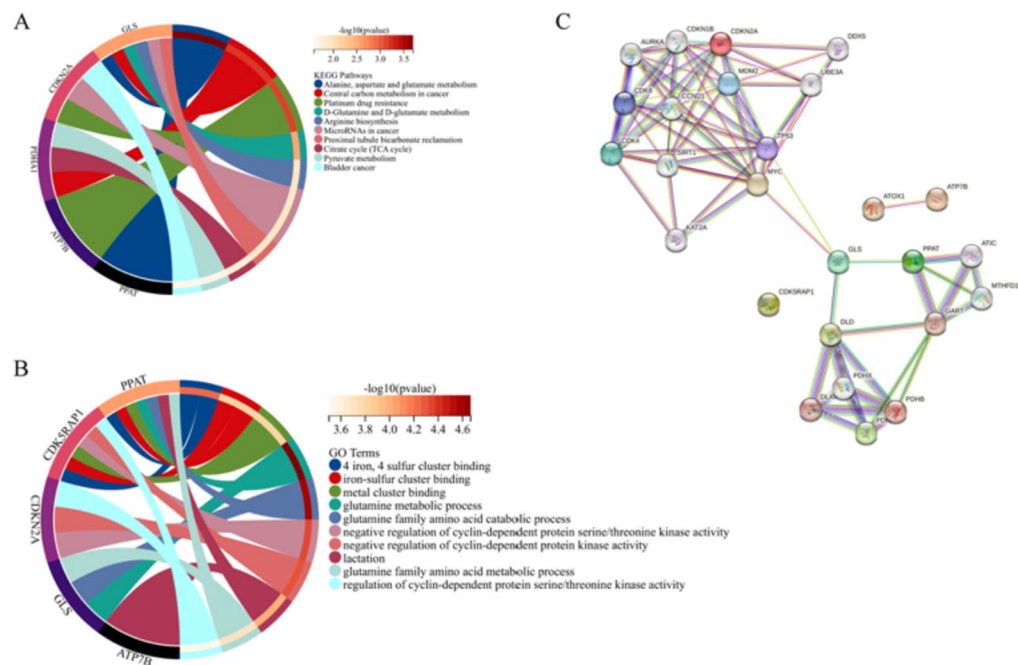


Fig. 8. 6 cuproptosis-related key genes co-expression network and functional enrichment. **(A).** KEGG Pathway of 6 cuproptosis-related key genes. **(B).** GO annotation of 6 cuproptosis-related key genes. **(C).** Protein-protein Interaction Enrichment Analysis shows the 6 cuproptosis-related key genes co-expression network.

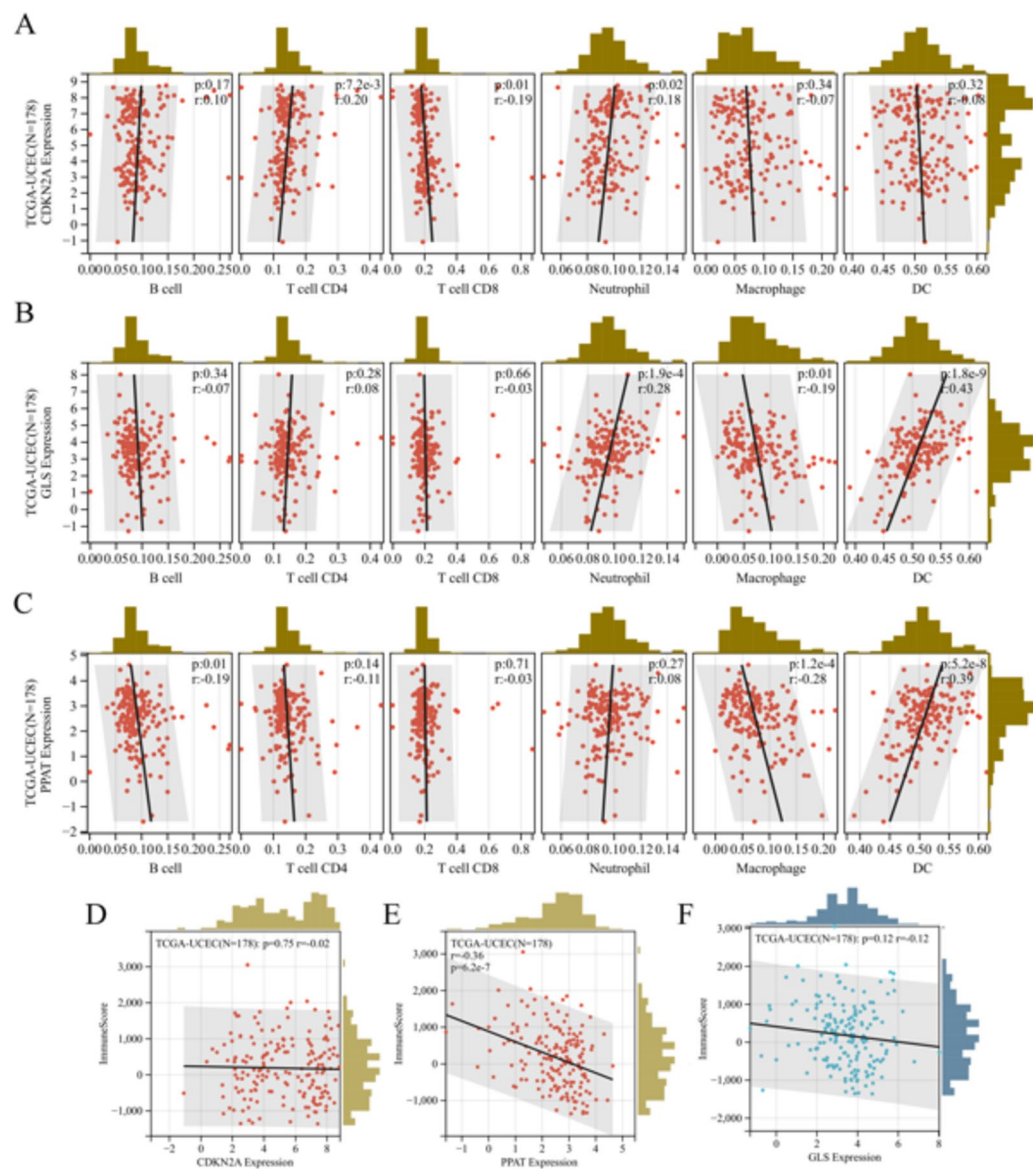


Fig. 9. Immune cell infiltration score and immune infiltration score for 3 cuproptosis-related genes. (A-C) B cell, T cell CD4, T cell CD8, Neutrophil, Macrophage, and DC infiltration scores of 3 cuproptosis-related genes. (D-F) Immune infiltration score of 3 cuproptosis-related genes.

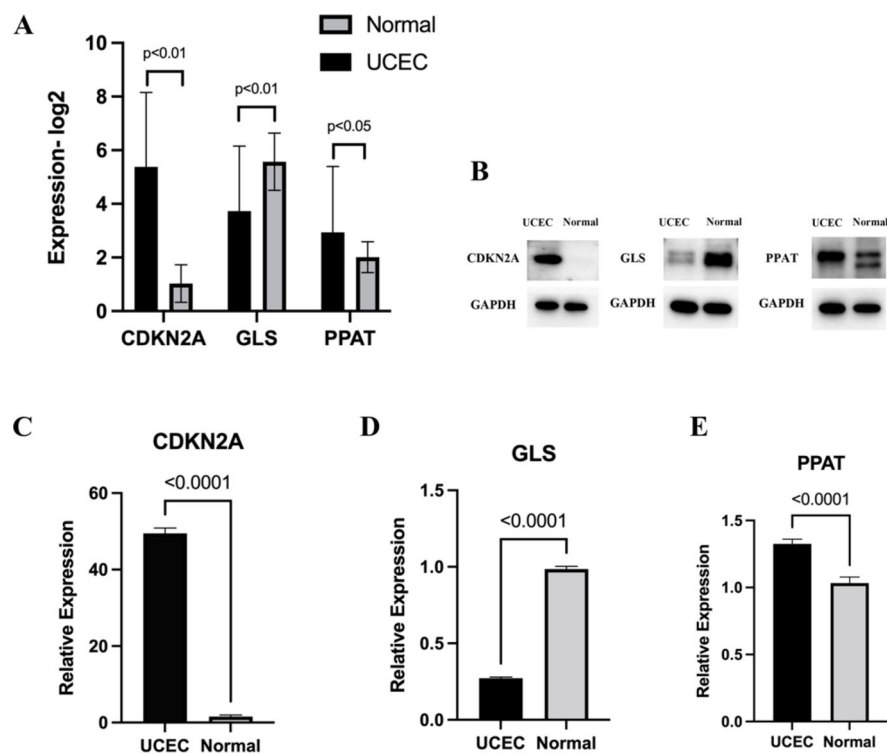


Fig. 10. The mRNA and protein level of the 3 cuproptosis-related genes in UCEC tissues and normal tissues. (A) mRNA levels of the 3 cuproptosis-related genes in 30 UCEC and normal endometrial tissues; (B-E) Protein level of 3 cuproptosis-related genes in 30 UCEC and normal endometrial tissues.

Data availability

The datasets generated and analysed during the current study are available in the TCGA database repository, <https://portal.gdc.cancer.gov/>.

Received: 19 January 2023; Accepted: 13 January 2025

Published online: 16 January 2025

References

- Chen, W. et al. Cancer statistics in China, 2015. *CA Cancer J. Clin.* 2016 Mar-Apr ;66(2):115–132. <https://doi.org/10.3322/caac.21338>
- Siegel, R. L., Miller, K. D., Fuchs, H. E., Jemal, A. & Cancer statistics CA Cancer J Clin. 2022;72(1):7–33. (2022). <https://doi.org/10.3322/caac.21708>
- Sung, H. et al. Global Cancer statistics 2020: GLOBOCAN estimates of incidence and Mortality Worldwide for 36 cancers in 185 countries. *CA Cancer J. Clin.* 71 (3), 209–249. <https://doi.org/10.3322/caac.21660> (2021).
- Lortet-Tieulent, J., Ferlay, J., Bray, F. & Jemal, A. International patterns and trends in Endometrial Cancer incidence, 1978–2013. *J. Natl. Cancer Inst.* 110 (4), 354–361. <https://doi.org/10.1093/jnci/djx214> (2018).
- Han, C. et al. Novel targeted therapies in ovarian and uterine carcinosarcomas. *Discov Med.* 25 (140), 309–319 (2018).
- Travaglino, A. et al. Impact of endometrial carcinoma histotype on the prognostic value of the TCGA molecular subgroups. *Arch. Gynecol. Obstet.* 301 (6), 1355–1363. <https://doi.org/10.1007/s00404-020-05542-1> (2020).
- Tang, D., Kang, R., Berghe, T. V., Vandenabeele, P. & Kroemer, G. The molecular machinery of regulated cell death. *Cell. Res.* 29 (5), 347–364. <https://doi.org/10.1038/s41422-019-0164-5> (2019).
- Tsvetkov, P. et al. Copper induces cell death by targeting lipoylated TCA cycle proteins. *Science* 375 (6586), 1254–1261. <https://doi.org/10.1126/science.abf0529> (2022).
- Vittinghoff, E. & McCulloch, C. E. Relaxing the rule of ten events per variable in logistic and Cox regression. *Am. J. Epidemiol.* 165 (6), 710–718. <https://doi.org/10.1093/aje/kwk052> (2007).
- Biau, D. J., Kernéis, S. & Porcher, R. Statistics in brief: the importance of sample size in the planning and interpretation of medical research. *Clin. Orthop. Relat. Res.* 466 (9), 2282–2288. <https://doi.org/10.1007/s11999-008-0346-9> (2008).
- Oliveri, V. Selective targeting of Cancer cells by copper ionophores: an overview. *Front. Mol. Biosci.* 9, 841814. <https://doi.org/10.3389/fmolb.2022.841814> (2022).
- Shao, S., Si, J. & Shen, Y. Copper as the target for anticancer nanomedicine[J]. *Adv. Ther.* 2 (5), 1800147 (2019).
- Lelièvre, P., Sancey, L., Coll, J. L., Deniaud, A. & Busser, B. The multifaceted roles of copper in Cancer: a Trace Metal element with Dysregulated Metabolism, but also a target or a bullet for Therapy. *Cancers (Basel)*. 12 (12), 3594. <https://doi.org/10.3390/cancers12123594> (2020).
- Li, Y. Copper homeostasis: an emerging target for cancer treatment. *IUBMB Life*. 72 (9), 1900–1908. <https://doi.org/10.1002/iub.2341> (2020).
- Shanbhag, V. C. et al. Copper metabolism as a unique vulnerability in cancer. *Biochim. Biophys. Acta Mol. Cell. Res.* 1868 (2), 118893. <https://doi.org/10.1016/j.bbamcr.2020.118893> (2021).
- Li, X. et al. Analysis of cuproptosis in hepatocellular carcinoma using multi-omics reveals a comprehensive HCC landscape and the immune patterns of cuproptosis. *Front. Oncol.* 12, 1009036. <https://doi.org/10.3389/fonc.2022.1009036> (2022).
- Song, Q., Zhou, R., Shu, F. & Fu, W. Cuproptosis scoring system to predict the clinical outcome and immune response in bladder cancer. *Front. Immunol.* 13, 958368. <https://doi.org/10.3389/fimmu.2022.958368> (2022).
- Liu, Q., Yu, M. & Zhang, T. Construction of oxidative stress-related genes risk Model predicts the prognosis of Uterine Corpus Endometrial Cancer patients. *Cancers (Basel)*. 14 (22), 5572. <https://doi.org/10.3390/cancers14225572> (2022).
- Zhang, J. et al. An integrated autophagy-related gene signature predicts prognosis in human endometrial cancer. *BMC Cancer*. 20 (1), 1030. <https://doi.org/10.1186/s12885-020-07535-4> (2020).
- Zhou, W. J. et al. Estrogen inhibits autophagy and promotes the growth of endometrial cancer by promoting glutamine metabolism. *Cell. Commun. Signal.* 17 (1), 99. <https://doi.org/10.1186/s12964-019-0412-9> (2019).
- Devis-Jauregui, L., Eritja, N., Davis, M. L., Matias-Guiu, X. & Llobet-Navàs, D. Autophagy in the physiological endometrium and cancer. *Autophagy* 17 (5), 1077–1095. <https://doi.org/10.1080/15548627.2020.1752548> (2021).
- Chen, Y. Identification and Validation of Cuproptosis-Related Prognostic Signature and Associated Regulatory Axis in Uterine Corpus Endometrial Carcinoma. *Front. Genet.* 13, 912037. <https://doi.org/10.3389/fgene.2022.912037> (2022).
- Wu, Q. et al. A comprehensive analysis focusing on cuproptosis to investigate its clinical and biological relevance in uterine corpus endometrial carcinoma and its potential in indicating prognosis. *Front. Mol. Biosci.* 9, 1048356. <https://doi.org/10.3389/fmolb.2022.1048356> (2022).
- Iasonos, A., Schrag, D., Raj, G. V. & Panageas, K. S. How to build and interpret a nomogram for cancer prognosis. *J. Clin. Oncol.* 26 (8), 1364–1370. <https://doi.org/10.1200/JCO.2007.12.9791> (2008).
- Langfelder, P. & Horvath, S. WGCNA: an R package for weighted correlation network analysis. *BMC Bioinform.* 9, 559. <https://doi.org/10.1186/1471-2105-9-559> (2008).

Acknowledgements

The authors thank the developers of Sanger box tools, a free online platform for data analysis (<http://vip.sangerbox.com/>).

Author contributions

Conceptualization: Jianqi Li; Formal analysis: Jianqi Li; Funding acquisition: Jianqi Li; Methodology: Yanfang Huang, Guoxian Luo and Xiujie Sheng; Software: Guoxian Luo; Writing – original draft: Yanfang Huang, Guoxian Luo, Xiujie Sheng and Jianqi Li; Writing – review & editing: Yanfang Huang, Guoxian Luo and Jianqi Li.

Funding

Not applicable.

Declarations

Competing interests

The authors declare no competing interests.

Consent for publication

Not applicable.

Ethics approval and consent to participate

Not Applicable.

Additional information

Supplementary Information The online version contains supplementary material available at <https://doi.org/10.1038/s41598-025-86756-8>.

Correspondence and requests for materials should be addressed to J.L.

Reprints and permissions information is available at www.nature.com/reprints.

Publisher's note Springer Nature remains neutral with regard to jurisdictional claims in published maps and institutional affiliations.

Open Access This article is licensed under a Creative Commons Attribution-NonCommercial-NoDerivatives 4.0 International License, which permits any non-commercial use, sharing, distribution and reproduction in any medium or format, as long as you give appropriate credit to the original author(s) and the source, provide a link to the Creative Commons licence, and indicate if you modified the licensed material. You do not have permission under this licence to share adapted material derived from this article or parts of it. The images or other third party material in this article are included in the article's Creative Commons licence, unless indicated otherwise in a credit line to the material. If material is not included in the article's Creative Commons licence and your intended use is not permitted by statutory regulation or exceeds the permitted use, you will need to obtain permission directly from the copyright holder. To view a copy of this licence, visit <http://creativecommons.org/licenses/by-nc-nd/4.0/>.

© The Author(s) 2025